

Magnetometry with entangled atomic samples

Vivi Petersen,^{1,2} Lars Bojer Madsen,² and Klaus Mølmer^{1,2}

¹*QUANTOP - Danish National Research Foundation Center for Quantum Optics*

²*Department of Physics and Astronomy, University of Aarhus, DK-8000 Århus C, Denmark*

(Dated: November 11, 2018)

We present a theory for the estimation of a scalar or a vector magnetic field by its influence on an ensemble of trapped spin polarized atoms. The atoms interact off-resonantly with a continuous laser field, and the measurement of the polarization rotation of the probe light, induced by the dispersive atom-light coupling, leads to spin-squeezing of the atomic sample which enables an estimate of the magnetic field which is more precise than that expected from standard counting statistics. For polarized light and polarized atoms, a description of the non-classical components of the collective spin angular momentum for the atoms and the collective Stokes vectors of the light-field in terms of effective gaussian position and momentum variables is practically exact. The gaussian formalism describes the dynamics of the system very effectively and accounts explicitly for the back-action on the atoms due to measurement and for the estimate of the magnetic field. Multi-component magnetic fields are estimated by the measurement of suitably chosen atomic observables and precision and efficiency is gained by dividing the atomic gas in two or more samples which are entangled by the dispersive atom-light interaction.

I. INTRODUCTION

Precision atomic magnetometry relies on the measurement of the Larmor precession of a spin-polarized atomic sample in a magnetic field [1, 2, 3]. From standard counting statistics arguments, one might expect the uncertainty in such measurements to decrease with the interaction time t and with the number of atoms N_{at} as $1/\sqrt{N_{\text{at}}t}$. If, on the other hand, the monitoring of the atomic sample, necessary for the read-out of the estimate of the magnetic field, squeezes the atomic spin, the above limit may be surpassed. In a recent theoretical analysis it was considered to estimate a scalar B field by a polarization rotation measurement of an off-resonant light beam passing through a trapped cloud of spin-1/2 atoms. This interaction squeezes the spin of the atomic sample, and by quantum trajectory theory [4] combined with the classical theory of Kalman filters [5, 6], the uncertainty in the field strength was found to decrease as $1/(N_{\text{at}}t^{3/2})$ [5]. Very recently this proposal was implemented experimentally, and indeed sub-shotnoise sensitivity was found [7].

In a recent analysis of the experiment, we advocated treating all variables, including the magnetic field, as quantum variables [8]. Secondly, we introduced a gaussian approximation at an early stage in the formulation of the theory. We further motivated and developed this point of view in a detailed discussion of the spin-squeezing process [9]. As mentioned in these works, the gaussian approximation is essentially exact for the atomic and photonic degrees of freedom of the system under concern, and the advantages obtained by introducing this description from the outset of the theoretical treatment are at least four-fold: (i) the gaussian description explicitly accounts for the dynamics of the system and its behavior under measurements through update formulae for the expectation values and the covariance matrix which together fully characterize the gaussian state, (ii) the numerical treatment of the update formulae involves

only the manipulation of low-dimensional matrices, (iii) in the limit of small time-steps the update formula for the covariance matrix translates into a matrix Riccati differential equation which often lends itself to analytical solution, and (iv) effects of noise introduced by, e.g., photon absorption and atomic decay are readily included.

Here, we extend our previous analysis [8] to explore the possibilities for estimating B fields with not only one, but also two or three spatial components. In cases with more than one component, it is advantageous to use two or more polarized atomic samples. With such setups, we may identify sets of commuting observables which allow a simultaneous estimate of the B field components. We also discuss how to gain precision and efficiency by entangling the atomic gasses.

The paper is organized as follows. In Sec. II, we introduce the atom-photon system used for the estimation of the magnetic field and describe the atomic and photonic gaussian variables. In Sec. III, we investigate the estimation of a single B field component, we describe our theoretical method in some detail and we derive an analytical solution for the decrease in variance of the B field as a function of time. In Sec. IV, we present our results for the estimation of two or three spatial B field components. In Sec. V, we quantify the entanglement between the samples used in our optimal protocol for the estimation of several B field components. In Sec. VI, we explain how to include noise in the description and we study the effects of noise on the precision of measurements. In Sec. VII, we conclude and present an outlook.

II. ATOM-LIGHT SYSTEM: COLLECTIVE VARIABLES

To estimate the strength of a B field, we let it interact with an atomic spin-system which is continuously probed by a light beam along the lines of Refs. [8, 9, 10, 11, 12,

13, 14]. In short, we imagine to have a gas of trapped spin-1/2 atoms which are described by a collective spin operator $\mathbf{J} = \frac{\hbar}{2} \sum_i \boldsymbol{\sigma}_i$ with $\boldsymbol{\sigma}_i$ the Pauli spin matrices. The atoms are initially pumped such that they are polarized along the x axis and J_x can be treated as a classical variable $\langle J_x \rangle = \frac{\hbar N_{\text{at}}}{2}$ with N_{at} the number of atoms. The other two projections of the spin, J_y and J_z , obey the commutation relation $[J_y, J_z] = i\hbar J_x$ which may be rewritten as $[x_{\text{at}}, p_{\text{at}}] = i$ for the effective position and momentum variables $x_{\text{at}} = \frac{J_y}{\sqrt{\hbar \langle J_x \rangle}}$, $p_{\text{at}} = \frac{J_z}{\sqrt{\hbar \langle J_x \rangle}}$. The uncertainty is easily shown to be minimal in the initial state and, hence, the state pertaining to x_{at} and p_{at} is gaussian.

The light beam propagates along the y axis and is linearly polarized along x such that its Stokes operator $\langle S_x \rangle = \frac{\hbar N_{\text{ph}}}{2}$ is classical with N_{ph} the number of photons. The two remaining components fulfill a commutator relation similar to the atomic spin case. Accordingly, for the effective variables $x_{\text{ph}} = \frac{S_y}{\sqrt{\hbar \langle S_x \rangle}}$, $p_{\text{ph}} = \frac{S_z}{\sqrt{\hbar \langle S_x \rangle}}$, we have $[x_{\text{ph}}, p_{\text{ph}}] = i$ and the initial coherent state of the field is a minimum uncertainty gaussian state.

As shown in Ref. [9] and references therein, the light and atomic variables evolve as

$$x_{\text{at}} \mapsto x_{\text{at}} + \kappa_\tau p_{\text{ph}}, \quad p_{\text{at}} \mapsto p_{\text{at}} \quad (1)$$

$$x_{\text{ph}} \mapsto \kappa_\tau p_{\text{at}} + x_{\text{ph}}, \quad p_{\text{ph}} \mapsto p_{\text{ph}} \quad (2)$$

when a segment of probe light of duration τ and flux Φ , and with a characteristic atom-light coupling $\kappa_\tau \propto \sqrt{\langle J_x \rangle \Phi \tau}$, is transmitted through the gas. The present dynamics in combination with a detection of the x_{ph} component of the photon field leads to squeezing of the p_{at} component of the atomic spin.

III. ESTIMATING ONE SPATIAL COMPONENT OF A MAGNETIC FIELD

The problem of estimating a single component of a B field was treated in Ref. [8] and only a brief discussion is included here for completeness. Figure 1 shows the setup. The B field directed along the y direction, causes

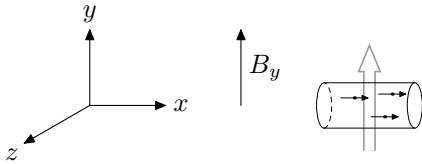


FIG. 1: Setup for measuring the B field component along the y axis. This is done using one atomic gas polarized along the x axis and one photon probe beam propagating along the y axis with a classical S_x .

a Larmor rotation of the atomic spin towards the z axis, i.e., in time τ , p_{at} evolves as $p_{\text{at}} \mapsto p_{\text{at}} - \mu_\tau B$ where μ_τ is given by the magnetic moment β , via $\mu_\tau = \frac{1}{\hbar} \beta \sqrt{\langle J_x \rangle} \tau$ [8].

Hence, Eqs. (1)–(2), generalize to

$$\mathbf{y} \mapsto \mathbf{S}_\tau \mathbf{y} \quad (3)$$

with $\mathbf{y} = (B_y, x_{\text{at}}, p_{\text{at}}, x_{\text{ph}}, p_{\text{ph}})^T$ and

$$\mathbf{S}_\tau = \begin{pmatrix} 1 & 0 & 0 & 0 & 0 \\ 0 & 1 & 0 & 0 & \kappa_\tau \\ -\mu_\tau & 0 & 1 & 0 & 0 \\ 0 & 0 & \kappa_\tau & 1 & 0 \\ 0 & 0 & 0 & 0 & 1 \end{pmatrix}. \quad (4)$$

It is the coupling of the B field to the spin-squeezed variable p_{at} that makes an improved precision measurement of the magnetic field possible [5].

Gaussian variables have been studied widely in relation to entanglement [15]. The gaussian description can be used as long as the interactions in the system are at most second order polynomials in the position and momentum operators and only homodyne measurements are carried out on the observables [16]. In particular, the operations of relevance for this work preserve the character of a gaussian state. We treat the continuous probe beam as a succession of small beam segments of duration τ , and let the state develop during time τ between successive measurements. We recall that a gaussian state is fully characterized by its mean value vector $\mathbf{m} = \langle \mathbf{y} \rangle$ and its covariance matrix $\boldsymbol{\gamma}$ where $\gamma_{ij} = 2\text{Re}(\langle (y_i - \langle y_i \rangle)(y_j - \langle y_j \rangle) \rangle)$. Accordingly, we only need update formulae for \mathbf{m} and $\boldsymbol{\gamma}$. The initial covariance matrix is $\boldsymbol{\gamma}_0 = \text{diag}(2\text{Var}(B_0), 1, 1, 1, 1)$ with $\text{Var}(B_0)$ the initial variance of the B field. Under the linear transformation (3), \mathbf{m} and $\boldsymbol{\gamma}$ transform as

$$\mathbf{m}(t + \tau) = \mathbf{S}_\tau \mathbf{m}(t) \quad (5)$$

$$\boldsymbol{\gamma}(t + \tau) = \mathbf{S}_\tau \boldsymbol{\gamma}(t) \mathbf{S}_\tau^T. \quad (6)$$

The photon field is monitored continuously by detection of x_{at} . A major advantage of the gaussian description is that the back-action on the residual system due to measurement is explicitly given. We write the covariance matrix as [16, 17, 18]

$$\boldsymbol{\gamma} = \begin{pmatrix} \mathbf{A}_\gamma & \mathbf{C}_\gamma \\ \mathbf{C}_\gamma^T & \mathbf{B}_\gamma \end{pmatrix}, \quad (7)$$

with \mathbf{A}_γ the covariance matrix for the B field and atoms, $\mathbf{y}_1 = (B_y, x_{\text{at}}, p_{\text{at}})^T$, \mathbf{B}_γ the covariance matrix for the photons, $\mathbf{y}_2 = (x_{\text{ph}}, p_{\text{ph}})^T$, and \mathbf{C}_γ the correlation matrix for \mathbf{y}_1 and \mathbf{y}_2 . The measurement of x_{ph} then transforms these matrices according to [17, 18]

$$\mathbf{A}_\gamma \mapsto \mathbf{A}_\gamma - \mathbf{C}_\gamma (\pi \mathbf{B}_\gamma \pi)^- \mathbf{C}_\gamma^T, \quad (8a)$$

$$\mathbf{B}_\gamma \mapsto \mathbb{1}_{2 \times 2}, \quad (8b)$$

$$\mathbf{C}_\gamma \mapsto 0, \quad (8c)$$

where $\pi = \text{diag}(1, 0)$, and $()^-$ denotes the Moore-Penrose pseudo-inverse. Equations (8b) and (8c) follow from the fact that a new light segment is used in every measurement: The initial covariance matrix for every new segment of a coherent photon beam is the identity matrix,

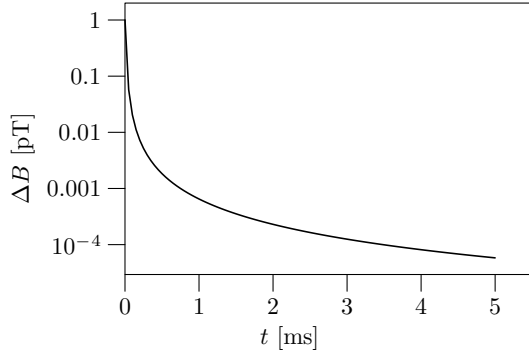


FIG. 2: Uncertainty of one B field component as a function of time. The value at $t = 5$ ms is $\Delta B_y = 5.814 \times 10^{-5}$ pT. We have chosen a segment duration $\tau = 10^{-8}$ s and corresponding field parameters $\kappa_\tau^2 = 0.0183$ and $\mu_\tau = 8.8 \times 10^{-4}$.

and immediately after measurement there are no correlations between \mathbf{y}_1 and \mathbf{y}_2 so \mathbf{C}_γ is substituted with the zero matrix.

The time evolution of \mathbf{m} depends on the actual measurements in the optical detection which is a random process. Therefore the time evolution of the mean value vector is a stochastic process, and it transforms as [8, 16, 17]

$$\mathbf{m}_1 \mapsto \mathbf{m}_1 + \mathbf{C}_\gamma (\pi \mathbf{B}_\gamma \pi)^-(\chi, \cdot)^T, \quad (9)$$

where χ is the difference between the measurement outcome and the expectation value of x_{ph} , i.e., a gaussian random variable with mean value zero and variance $1/2$. Since $(\pi \mathbf{B}_\gamma \pi)^- = \text{diag}(B_{11}^{-1}, 0)$ with B_{11} twice the variance of x_{ph} , the second entrance in the vector (χ, \cdot) need not be specified. In closing this section, we note that it is possible to understand the transformations in Eqs. (8a) and (9) by the corresponding transformation of classical gaussian probability distributions [9, 19].

A. Analytical solution

From the update formulae, we may, in the limit of small time increments, derive a differential equation for \mathbf{A}_γ . As B_y only causes rotation perpendicular to its direction, the variable $x_{\text{at}} \propto J_y$ does not couple to (B_y, p_{at}) and, hence, we only need to consider a 2×2 system with $\mathbf{y} = (B_y, p_{\text{at}})^T$. The pertaining differential equation is on the matrix Ricatti form [20]

$$\dot{\mathbf{A}}_\gamma(t) = \mathbf{C} - \mathbf{D}\mathbf{A}_\gamma(t) - \mathbf{A}_\gamma(t)\mathbf{E} - \mathbf{A}_\gamma(t)\mathbf{B}\mathbf{A}_\gamma(t), \quad (10)$$

with $\mathbf{C} = 0$, $\mathbf{D} = \begin{pmatrix} 0 & 0 \\ \mu & 0 \end{pmatrix}$, $\mathbf{E} = \mathbf{D}^T$, and $\mathbf{B} = \begin{pmatrix} 0 & 0 \\ 0 & \kappa^2 \end{pmatrix}$ where $\kappa^2 = \kappa_\tau^2/\tau$ and $\mu = \mu_\tau/\tau$. As may be checked by insertion, the solution to Eq. (10) is $\mathbf{A}_\gamma = \mathbf{W}\mathbf{U}^{-1}$, where $\dot{\mathbf{W}} = -\mathbf{D}\mathbf{W} + \mathbf{C}\mathbf{U}$ and $\dot{\mathbf{U}} = \mathbf{B}\mathbf{W} + \mathbf{E}\mathbf{U}$. The linear differential equations for \mathbf{W}, \mathbf{U} can be solved, and

the resulting solution for the variance of the B field reads:

$$\begin{aligned} \text{Var}(B(t)) &= \frac{\text{Var}(B_0)(\kappa^2 t + 1)}{\frac{1}{6}\kappa^4 \mu^2 \text{Var}(B_0)t^4 + \frac{2}{3}\kappa^2 \mu^2 \text{Var}(B_0)t^3 + \kappa^2 t + 1} \\ &\xrightarrow{t \rightarrow \infty} \frac{6}{\kappa^2 \mu^2 t^3} \propto \frac{1}{N_{\text{at}}^2 \Phi t^3}, \end{aligned} \quad (11)$$

where we have introduced the photon flux Φ .

Figure 2 shows the decrease in the uncertainty of the B field with time in a calculation with physically realizable parameters. From standard counting statistics one might have expected the variance to decrease as $1/N_{\text{at}}$. Due to the measurement-induced squeezing of the atomic spin, we do, however, obtain the faster $1/N_{\text{at}}^2$ decrease. As we shall discuss in Sec. VI, the inclusion of noise due to decoherence of atomic spins will alter this dependence on time and on the number of atoms.

IV. ESTIMATING TWO OR THREE SPATIAL COMPONENTS OF A MAGNETIC FIELD

In this section, we describe how to estimate two or three spatial components of a B field. In the setup in Fig. 1, we obtained an estimate of one component by using one atomic gas and one probe beam. To estimate more components we shall need more probe beams and more atomic gasses.

In order to make a fair comparison of different schemes, we shall assume that all measurements are carried out in a time interval of the same duration, e.g., 5 ms as in Fig. 2, and that the total photon number used and the total number of atoms are kept constant.

A. Two components: two probe beams and one or two separate atomic gasses

In order to estimate B_z in addition to B_y , we observe that B_z causes a rotation of $x_{\text{at}} \propto J_y$ so if we add a second optical probe beam propagating along z in Fig. 1 and with S_x classical then x_{at} will cause a rotation of the field variable $p_{\text{ph}} \propto S_z$ on the second beam which we can then measure. The setup is symmetric with respect to y and z , and we obtain equal uncertainties on B_y and B_z . The problem with this approach is that unlike the unknown classical quantities B_y and B_z , the atomic observables x_{at} and p_{at} do not commute. While the first beam squeezes x_{at} , it anti-squeezes p_{at} , and the other beam does the opposite. Thus effectively we have no squeezing of the atoms leaving us with the $1/t$ decrease in the variance of the B components as shown in Fig. 3.

To estimate simultaneously and precisely two B field components we need to measure two commuting atomic variables. Such a measurement is possible by using two separate gasses and by estimating one B field component

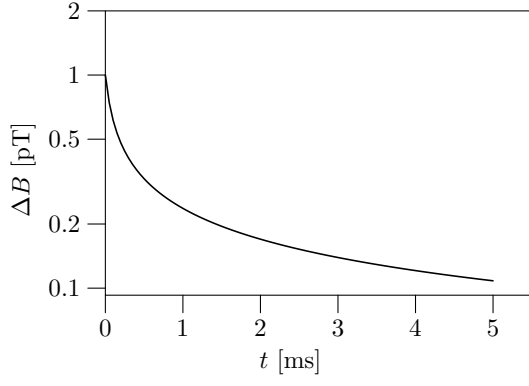


FIG. 3: Uncertainty of two B field components as a function of time. We use a single atomic gas and two probe beams which are turned on simultaneously. We have chosen a segment duration $\tau = 10^{-8}$ s and corresponding field parameters $\kappa_\tau^2 = 0.0183$ and $\mu_\tau = 8.8 \times 10^{-4}$. The joint uncertainty of the two B fields at $t = 5$ ms is $\Delta B_y = \Delta B_z = 0.1083$ pT.

on each system with individual probe beams. Both systems are then equivalent to the setup in Fig. 1 used to measure B_y , but in one system (not shown), the probe beam propagates along the z axis such that we estimate B_z by measuring p_{ph} . The result is similar to the result in Fig. 2 except that the number of atoms and the photon flux are both divided by two as they are shared between the two systems. The uncertainty of the B fields for large t is proportional to $1/\sqrt{N_{\text{at}}^2 \Phi t^3}$ so the uncertainty for estimating two B field components is $2\sqrt{2}$ times larger than if we had measured only one with the same field and atomic resources.

The achievements of a sequential measurement of first B_y and then B_z are shown in Fig. 4. In the first half of the time the full photon flux is spent to measure B_y , leaving the uncertainty about B_z unchanged. Although B_z is subsequently coupled to an anti-squeezed atomic component, it is quickly squeezed, and the estimate of B_z shows a $1/\sqrt{N_{\text{at}}^2 \Phi t^3}$ dependence as in Eq. (11). Now the other atomic observable is anti-squeezed, but this will surely not degrade our information already obtained about the classical B_y component. The values of $\text{Var}(B_y(t))$ and $\text{Var}(B_z(t))$ are $2\sqrt{2}$ times larger than the uncertainty reported in Fig. 2 because only half the time is spent on the measurement of each component.

B. Two components: two entangled gasses and two probe beams

If we split the atomic sample into two and polarize one gas along x and the other along $-x$ such that $\langle J_{x_1} \rangle = -\langle J_{x_2} \rangle$, then the two observables $(J_{y_1} - J_{y_2})$ and $(J_{z_1} - J_{z_2})$, and equivalently $x_{\text{at}_1} - x_{\text{at}_2}$ and $p_{\text{at}_1} - p_{\text{at}_2}$ commute. We couple these observables to the B fields and probe beams and use the setup shown in Fig. 5 (see also the entanglement experiment of Ref. [12]).

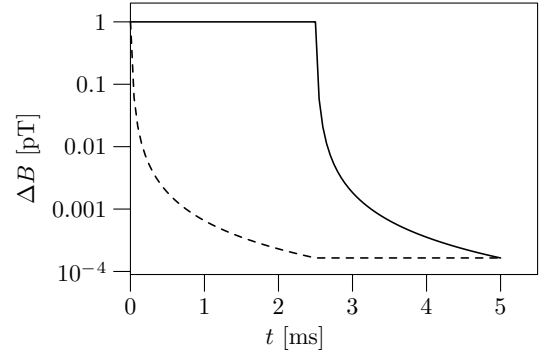


FIG. 4: Uncertainty of two B field components as a function of time using one atomic gas. B_y is estimated in the first half of the time and B_z in the second half. The dashed line is for B_y and the value at $t = 5$ ms is $\Delta B_y = 1.647 \times 10^{-4}$ pT. The full line is for B_z and the value at $t = 5$ ms is $\Delta B_z = 1.645 \times 10^{-4}$ pT. We have chosen a segment duration $\tau = 10^{-8}$ s and corresponding field parameters $\kappa_\tau^2 = 0.0183$ and $\mu_\tau = 8.8 \times 10^{-4}$.

Both optical probe beams have S_x classical, and one beam propagates along y , the other along z . The beams

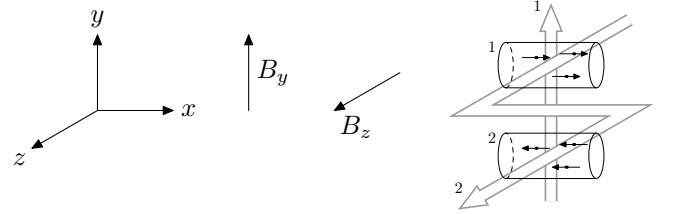


FIG. 5: Setup for measuring two components of a B field using two entangled gasses and two probe beams.

pass through both gasses and, oppositely to the protocol in the previous section, we use all atoms to estimate the B field components. The effective Hamiltonian for the setup is

$$\begin{aligned} \mathcal{H}_{\text{int}}\tau = & \mu_\tau B_y(x_{\text{at}_1} + x_{\text{at}_2}) + \mu_\tau B_z(p_{\text{at}_1} + p_{\text{at}_2}) \\ & + \kappa_\tau(p_{\text{at}_1} - p_{\text{at}_2})p_{\text{ph}_1} + \kappa_\tau(x_{\text{at}_1} - x_{\text{at}_2})x_{\text{ph}_2}, \end{aligned} \quad (12)$$

where the two minus signs can be implemented by changing the sign on κ_τ after the probe beams have passed through the first gas. In practice the change in sign can be effectuated by changing the sign of the detuning or by interchanging σ^+ and σ^- polarizations with, e.g., a half-wave-plate [21]. The gaussian state vector is $\mathbf{y} = (B_z, B_y, x_{\text{at}_1}, p_{\text{at}_1}, x_{\text{at}_2}, p_{\text{at}_2}, x_{\text{ph}_1}, p_{\text{ph}_1}, x_{\text{ph}_2}, p_{\text{ph}_2})^T$ and from the Heisenberg equations of motion for the op-

erators we get the following transformation matrix

$$\mathbf{S}_\tau = \begin{pmatrix} 1 & 0 & 0 & 0 & 0 & 0 & 0 & 0 & 0 & 0 \\ 0 & 1 & 0 & 0 & 0 & 0 & 0 & 0 & 0 & 0 \\ \mu & 0 & 1 & 0 & 0 & 0 & 0 & \kappa & 0 & 0 \\ 0 & -\mu & 0 & 1 & 0 & 0 & 0 & 0 & -\kappa & 0 \\ -\mu & 0 & 0 & 0 & 1 & 0 & 0 & \kappa & 0 & 0 \\ 0 & \mu & 0 & 0 & 0 & 1 & 0 & 0 & -\kappa & 0 \\ 0 & 0 & 0 & \kappa & 0 & -\kappa & 1 & 0 & 0 & 0 \\ 0 & 0 & 0 & 0 & 0 & 0 & 0 & 1 & 0 & 0 \\ 0 & 0 & 0 & 0 & 0 & 0 & 0 & 0 & 1 & 0 \\ 0 & 0 & -\kappa & 0 & \kappa & 0 & 0 & 0 & 0 & 1 \end{pmatrix}. \quad (13)$$

The time evolution of the uncertainty of the B fields is shown in Fig. 6. The final uncertainty of B_y and B_z is a factor $\sqrt{2}$ higher than in Fig. 2, where we used the entire photon flux to probe only a single B field component, but a factor of two lower than in the setup with separate probing of non-entangled gasses. These factors were expected because of the $1/\sqrt{N_{\text{at}}^2 \Phi t^3}$ dependence of Eq. (11). By using entangled gasses we use all atoms, but only half

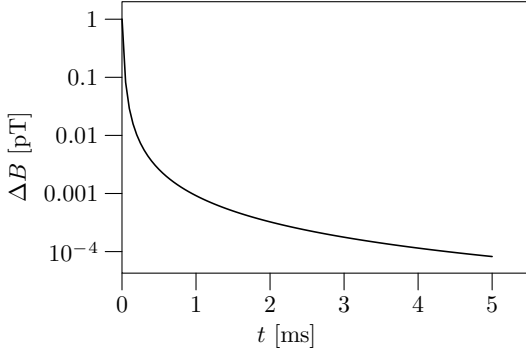


FIG. 6: Uncertainty of two B field components as a function of time using two atomic entangled gasses and two probe beams. We have chosen a segment duration $\tau = 10^{-8}$ s and corresponding field parameters $\kappa_\tau^2 = 0.0183$ and $\mu_\tau = 8.8 \times 10^{-4}$. The uncertainty at $t = 5$ ms is $\Delta B_y = \Delta B_z = 8.221 \times 10^{-5}$ pT.

of the photon flux to estimate each B field component.

C. Three dimensional vector magnetometry

For the estimation of three components of a magnetic field, the situation changes since a spin polarized sample is not a probe for the field component parallel with the spin. For the sequential probing one would thus measure B_y and B_z as just described, but one would have to rotate the sample by 90° to determine the last component B_x , and the errors of such a rotation will limit the precision.

As an alternative, we can divide the gas into three samples which are spin polarized along different directions. With such a setup, we can perform independent estimates of the three components. Since each component is determined by one third of the atoms and one

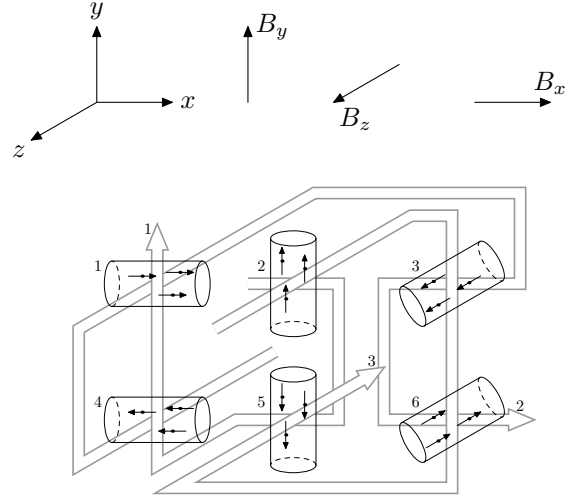


FIG. 7: Setup used to obtain estimates of all three components of a magnetic field. We use six atomic gasses and three probe beams.

third of the photons the scaling of Eq. (11) predicts that the uncertainty is a factor of $3\sqrt{3}$ larger than in Fig. 2 where we only estimated one B field component.

We wish to couple the B field components to three *commuting* atomic operators, involving as many atoms as possible, and a better, but also more complicated, setup is shown in Fig. 7. Here we use six entangled gasses and we let three probe beams pass through four gasses each. The gasses are polarized with the following macroscopic components: $\langle J_{x_1} \rangle = -\langle J_{x_4} \rangle$, $\langle J_{y_2} \rangle = -\langle J_{y_5} \rangle$, and $\langle J_{z_3} \rangle = -\langle J_{z_6} \rangle$. The optical fields are linearly polarized with macroscopic Stokes parameters $\langle S_{z_1} \rangle$, $\langle S_{y_2} \rangle$, and $\langle S_{x_3} \rangle$. The Hamiltonian for the system shown in Fig. 7 is given by

$$\begin{aligned} \mathcal{H}_{\text{int}} \tau \sqrt{\hbar \langle J_{x_1} \rangle} = & \mu_\tau (J_{x_2} + J_{x_3} + J_{x_5} + J_{x_6}) B_x \\ & + \mu_\tau (J_{y_1} + J_{y_3} + J_{y_4} + J_{y_6}) B_y \\ & + \mu_\tau (J_{z_1} + J_{z_2} + J_{z_4} + J_{z_5}) B_z \\ & + \kappa_\tau (J_{z_2} - J_{y_3} - J_{z_5} + J_{y_6}) S_3 \\ & + \kappa_\tau (J_{z_1} - J_{x_3} - J_{z_4} + J_{x_6}) S_2 \\ & + \kappa_\tau (J_{y_1} - J_{x_2} - J_{y_4} + J_{x_5}) S_1, \end{aligned} \quad (14)$$

Terms like $\mu_\tau J_{x_1} B_x$, which couple the classical components of the atomic spins to the B fields, are omitted from the interaction Hamiltonian as they do not contribute to the interactions to the same order, e.g., $[J_{y_1}, \mu_\tau J_{x_1} B_x] = -i\mu_\tau \hbar J_{z_1} B_x$, the product of two small quantities. By using the Hamiltonian of Eq. (14) we measure three commuting observables $J_{z_2} - J_{y_3} - J_{z_5} + J_{y_6}$, $J_{z_1} - J_{x_3} - J_{z_4} + J_{x_6}$, and $J_{y_1} - J_{x_2} - J_{y_4} + J_{x_5}$ and from their commutators with the Larmor term in Eq. (14), we see that they evolve in direct proportion with the three B field components.

The uncertainty of the B field components is shown as a function of time in Fig. 8. As we use $4/6$ of the atoms

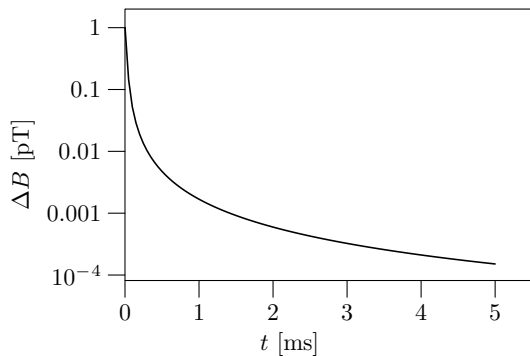


FIG. 8: Uncertainty of three B field components using six entangled gasses and three probe beams. We have chosen a segment duration $\tau = 10^{-8}$ s and corresponding field parameters $\kappa_\tau^2 = 0.0183$ and $\mu_\tau = 8.8 \times 10^{-4}$. The uncertainties at $t = 5$ ms are $\Delta B_x = \Delta B_y = \Delta B_z = 1.510 \times 10^{-4}$ pT.

and $1/3$ of the photon flux to estimate each B field component, the value of the uncertainty at $t = 5$ ms is $3\sqrt{3}/2$ times larger than if we use all atoms and all photons to estimate only one B field component and a factor of two smaller than if we use three separate systems to estimate the three B field components.

V. QUANTIFYING ENTANGLEMENT BETWEEN ATOMIC SAMPLES

To measure two or three B field components most efficiently, we showed that one should use entangled gasses. Here we quantify the degree of entanglement by calculating the gaussian entanglement of formation (GEoF) [22] from the covariance matrix of the atoms γ_{atoms} . Every time we apply the update formula, we may extract γ_{atoms} for a pair of gasses from our numerical procedure and up to local unitary operations this matrix turns out to be on the form

$$\gamma_{\text{atoms}} = \begin{pmatrix} n & 0 & k_x & 0 \\ 0 & n & 0 & -k_p \\ k_x & 0 & n & 0 \\ 0 & -k_p & 0 & n \end{pmatrix} \quad (15)$$

where n , k_x , and k_p ($k_x = k_p$, in our case) are the quantities of interest for the evaluation of the GEoF, $E = c_+(\Delta) \log[c_+(\Delta)] - c_-(\Delta) \log[c_-(\Delta)]$, with $c_\pm(\Delta) = \frac{1}{4}(\Delta^{-1/2} \pm \Delta^{1/2})^2$, and $\Delta = \min\left(1, \sqrt{(n - k_x)(n - k_p)}\right)$.

The GEoF for the two gasses used to estimate two B field components is shown in Fig. 9. For three B field components, we used six atomic gasses, and we have calculated the GEoF between different pairs of the gasses. Figure 10 shows the GEoF between two gasses polarized in opposite directions, e.g., gas number 1 and 4 in Fig. 8. The GEoF between pairs like 1 and 2 is zero.

The setup with two gasses is quite equivalent to the one implemented in recent entanglement experiments [12] except that the atomic systems are under the additional

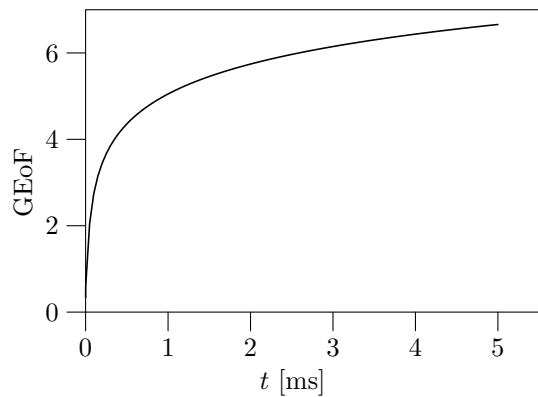


FIG. 9: GEoF for two entangled gasses corresponding to the case considered in Fig. 6.

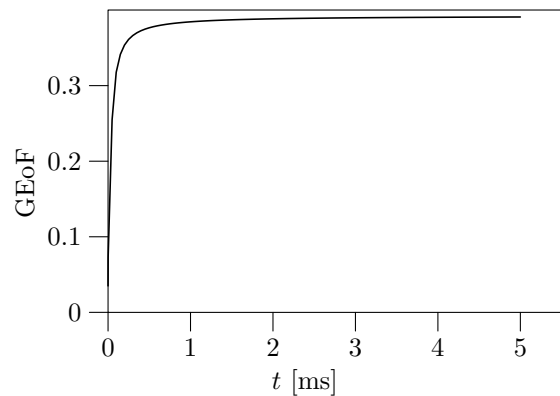


FIG. 10: GEoF for two gasses polarized in opposite directions as considered in Fig. 8.

influence of an initially unknown B field. This slows down the initial rate of generation of entanglement, but as $\text{Var}(B(t))$ approaches zero, the entanglement grows without limits as long as absorption and atomic decay can be neglected [23]. In the case of six gasses which are probed in a non-symmetric way, some pairs show entanglement and some do not. This can be understood by identification of operators that do not couple to the probe fields. The convergence of the entanglement between oppositely polarized gasses towards a constant value is also observed without coupling to a B field, and it is due to the incompleteness of the measurements on the pair by fields that also couple to other pairs of gasses. In symmetric setups with multiple gaussian variables, the theoretical maximum of pairwise entanglement between systems also have upper limits reflecting the impossibility for a quantum system to be maximally entangled with several other quantum systems at the same time [24, 25].

VI. EFFECTS OF NOISE

Effects of noise were recently discussed in Ref. [3]. Here we include noise in our gaussian description. As the photonic probe beams pass through the atomic sample, there is a probability for photon absorption [26] $\epsilon = N_{\text{at}} \frac{\sigma}{A} \frac{r^2/4}{r^2/4 + \Delta^2}$ and a related probability of atomic decay [8, 26] $\eta_\tau = \Phi \tau \frac{\sigma}{A} \frac{r^2/4}{r^2/4 + \Delta^2}$, where Γ is the atomic decay rate, $\sigma = \lambda^2/(2\pi)$ is the resonant photon absorption cross-section, A is the beam cross-section, and Δ the detuning. These processes lead to a reduction in the polarization of the Stokes vector and the atomic spin and to an incoherent noise contribution. These features were discussed in Refs. [8, 26] and at length in Ref. [9] so here it is sufficient to recall the generalizations of the update formulae in Eqs. (5)–(6):

$$\mathbf{m}(t + \tau) = \mathbf{L}_\tau \mathbf{S}_\tau \mathbf{m}(t) \quad (16)$$

$$\gamma(t + \tau) = \mathbf{L}_\tau \mathbf{S}_\tau \gamma(t) \mathbf{S}_\tau^T \mathbf{L}_\tau + \frac{\hbar N_{\text{at}}}{\langle J_x(t) \rangle} \mathbf{M}_\tau + \frac{\hbar N_{\text{ph}}}{2 \langle S_x(t) \rangle} \mathbf{N}, \quad (17)$$

where the diagonal matrices $\mathbf{L}_\tau = \text{diag}(1, \sqrt{1 - \eta_\tau}, \sqrt{1 - \eta_\tau}, \sqrt{1 - \epsilon}, \sqrt{1 - \epsilon})$, $\mathbf{M}_\tau = \text{diag}(0, \eta_\tau, \eta_\tau, 0, 0)$ and $\mathbf{N} = \text{diag}(0, 0, 0, \epsilon, \epsilon)$ describe the loss of polarization, and the noise introduced by stimulated emission and photon absorption, respectively. In each time step τ the atomic polarization $\langle J_x \rangle$ is reduced by the factor $(1 - \eta_\tau)$ and κ_τ is reduced by $\sqrt{1 - \eta_\tau}$. The presence of noise leaves the update formula for measurements in Eq. (8) unchanged. We may analyze the pertaining Riccati equation, which with $\mathbf{y} = (B, p_{\text{at}})^T$ can be written on the same form as in Eq. (10) but now with $\mathbf{C} = \begin{pmatrix} 0 & 0 \\ 0 & \frac{N_{\text{at}}}{\langle J_x(t) \rangle} \eta \end{pmatrix}$, $\mathbf{D} = \begin{pmatrix} 0 & 0 \\ \mu & \frac{\sigma}{2} \end{pmatrix}$, $\mathbf{E} = \mathbf{D}^T$, and $\mathbf{B} = \begin{pmatrix} 0 & 0 \\ 0 & \frac{(1 - \epsilon) \kappa^2(t)}{1 - \epsilon(1 - \frac{N_{\text{ph}}}{2 \langle S_x(t) \rangle})} \end{pmatrix}$, where $\eta = \eta_\tau/\tau$. One can show that the noise terms in \mathbf{D} and \mathbf{E} will have vanishing effect, and if we restrict ourselves to times corresponding to $\eta t \ll 1$, we may neglect the time dependence of $\langle J_x \rangle$, $\langle S_x \rangle$, and κ such that $N_{\text{at}}/\langle J_x \rangle = 2$, $N_{\text{ph}}/\langle S_x \rangle = 2$, and $\kappa(t) = \kappa(0)$. With these approximations, the resulting linear equations for the matrices \mathbf{U} and \mathbf{W} can be solved analytically, leading to lengthy expressions with sums of products of exponential functions, constant terms, and terms linear in time t . In the limit $\sqrt{\eta \kappa^2 t} \gg 1$, it is an accurate approximation to maintain only the leading exponential and we find

$$\text{Var}(B(t)) \rightarrow \frac{\eta}{\mu^2 t}. \quad (18)$$

Compared with the result in Eq. (11), we note that in the long time limit the uncertainty decreases as $1/N_{\text{at}} t$, and not as $1/N_{\text{at}}^2 t^3$ as in the noise-less case.

Figure 11 shows (solid line) the time evolution of the uncertainty of the B field. For short times the analytical expression (11) disregarding the noise (dotted line) in

the figure, is a good approximation, and for long times the numerical result follows the expression (18), shown as a dashed curve on the interval between 0.5 ms and 5 ms. Similar results are obtained in the simulation of measurements of two and three B field components.

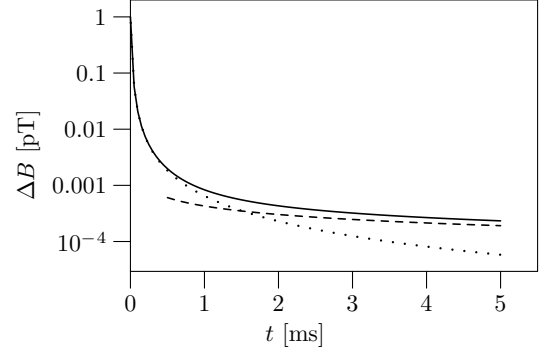


FIG. 11: Uncertainty of one B field component as a function of time. The full line is the result of a full numerical calculation and the value at $t = 5$ ms is $\Delta B_y = 2.333 \times 10^{-4}$ pT. The dotted line is without inclusion of noise and the value at $t = 5$ ms is $\Delta B_y = 5.814 \times 10^{-5}$ pT. We have chosen a segment duration $\tau = 10^{-8}$ s and corresponding field and noise parameters $\kappa_\tau^2 = 0.0183$, $\mu_\tau = 8.8 \times 10^{-4}$, $\eta_\tau = 1.76 \times 10^{-8}$ and $\epsilon = 0.0281$. The dashed curve shows the result of Eq. (18) valid for $t \ll 1$ s, and $\sqrt{\eta \kappa^2 t} \gg 1$.

VII. CONCLUSION AND OUTLOOK

We have considered how to estimate a vector magnetic field using a gaussian description of the variables describing the system. To estimate more than one field component it is fruitful to use pairwise entangled separate gasses. In other applications, e.g. teleportation, shared entanglement over some distance is a useful resource. We showed that entanglement can be a useful local resource to improve the accuracy in measurements and parameter estimation. We note that our protocol for the estimation of two B field components using two optical probe beams and two entangled gasses is experimentally very feasible. Essentially, it would require a combination of the magnetometry setup of Ref. [7] and the entanglement setup of Ref. [12].

In a broader perspective, the present work brings out the virtues of the gaussian state formalism when it comes not only to the detailed characterization of entanglement (see, e.g., Refs. [15, 16, 17, 18] and references therein), but also to the practical description of quantum systems [8, 9, 26]. The fact that the gaussian state is fully characterized in terms of its expectation value vector and covariance matrix means that the theory is easy to formulate and to evaluate. It is an outstanding advantage of the gaussian state description that explicit update formulae exist not only for the interaction dynamics but also for the back-action due to measurement. The gaussian

state description is a very versatile tool and we foresee this approach to be used for the description of a variety of different systems in the near future.

Acknowledgments

L.B.M. is supported by the Danish Natural Science Research Council (Grant No. 21-03-0163).

-
- [1] D. Budker, W. Gawlik, D. F. Kimball, S. M. Rochester, V. V. Yashchuk, and A. Weis, *Rev. Mod. Phys.* **74**, 1153 (2002).
 - [2] I. K. Kominis, T. W. Kornack, J. C. Allred, and M. V. Romalis, *Nature (London)* **422**, 596 (2003).
 - [3] M. Auzinsh, D. Budker, D. F. Kimball, S. M. Rochester, J. E. Stalnaker, A. O. Sushkov, and V. V. Yashchuk, *Can a quantum nondemolition measurement improve the sensitivity of an atomic magnetometer?*, physics/0403097 (2004).
 - [4] H. Carmichael, *An Open Systems Approach to Quantum Optics* (Springer-Verlag, Berlin Heidelberg, 1993).
 - [5] J. M. Geremia, J. K. Stockton, A. C. Doherty, and H. Mabuchi, *Phys. Rev. Lett.* **91**, 250801 (2003).
 - [6] J. K. Stockton, J. M. Geremia, A. C. Doherty, and H. Mabuchi, *Phys. Rev. A* **69**, 032109 (2004).
 - [7] J. M. Geremia, J. K. Stockton, and H. Mabuchi, *Sub-shotnoise atomic magnetometry*, quant-ph/0401107 (2004).
 - [8] K. Mølmer and L. B. Madsen, *Estimation of a classical parameter with gaussian probes: Magnetometry with collective atomic spins*, quant-ph/0402158 (2004), *Phys. Rev. A*, at print.
 - [9] L. B. Madsen and K. Mølmer, *Spin squeezing and precision probing with light and samples of atoms in the gaussian approximation*, quant-ph/0406146 (2004), *Phys. Rev. A*, at print.
 - [10] A. Kuzmich, N. P. Bigelow, and L. Mandel, *Europhys. Lett.* **42**, 481 (1998).
 - [11] L.-M. Duan, J. I. Cirac, P. Zoller, and E. S. Polzik, *Phys. Rev. Lett.* **85**, 5643 (2000).
 - [12] B. Julsgaard, A. Kozhekin, and E. S. Polzik, *Nature (London)* **413**, 400 (2001).
 - [13] Y. Takahashi, K. Honda, N. Tanaka, K. Toyoda, K. Ishikawa, and T. Yabuzaki, *Phys. Rev. A* **60**, 4974 (1999).
 - [14] A. Kuzmich, L. Mandel, J. Janis, Y. E. Young, R. Egnis-man, and N. P. Bigelow, *Phys. Rev. A* **60**, 2346 (1999).
 - [15] G. Giedke, J. Eisert, J. I. Cirac, and M. B. Plenio, *Entanglement transformations of pure gaussian states*, quant-ph/0301038 (2003).
 - [16] G. Giedke and J. I. Cirac, *Phys. Rev. A* **66**, 032316 (2002).
 - [17] J. Fiurášek, *Phys. Rev. Lett.* **89**, 137904 (2002).
 - [18] J. Eisert and M. B. Plenio, *Introduction to the basics of entanglement theory in continuous-variable systems*, quant-ph/0312071 (2003).
 - [19] P. S. Maybeck, *Stochastic Models, Estimation and Control*, vol. 1 of *Mathematics in Science and Engineering, Volume 141* (Academic Press, New York, 1979).
 - [20] J. K. Stockton, J. M. Geremia, A. C. Doherty, and H. Mabuchi, *Robust quantum parameter estimation: Coherent magnetometry with feedback*, quant-ph/0309101 (2003).
 - [21] W. A. Shurcliff, *Polarized Light* (Harvard University Press, Cambridge, 1962).
 - [22] G. Giedke, M. M. Wolf, O. Krüger, R. F. Werner, and J. I. Cirac, *Phys. Rev. Lett.* **91**, 107901 (2003).
 - [23] J. Sherson and K. Mølmer, *In preparation* (2004).
 - [24] M. M. Wolf, F. Verstraete, and J. I. Cirac, *Phys. Rev. Lett.* **92**, 087903 (2004).
 - [25] M. B. Plenio, J. Eisert, J. Dreißig, and M. Cramer, *Entropy, entanglement, and area: analytical results for harmonic lattice systems*, quant-ph/0405142 (2004).
 - [26] K. Hammerer, K. Mølmer, E. S. Polzik, and J. I. Cirac, *Light-matter quantum interface*, quant-ph/0312156 (2003), *Phys. Rev. A*, at print.